Published in ACS Applied Materials and Interfaces (ACS Appl. Mater. Interfaces 2021, 13, 26102−26108), which should be cited to refer to this work.

Molten Salt Templated Synthesis of Covalent Isocyanurate Frameworks with Tunable Morphology and High CO_2 Uptake Capacity

Kyung Seob Song, Siddulu Naidu Talapaneni, Timur Ashirov, and Ali Coskun*

ABSTRACT: The use of reactive molten salts, i.e., $ZnCl_2$, as a soft template and a catalyst has been actively investigated in the preparation of covalent triazine frameworks (CTFs). Although the soft templating effect of the salt melt is more prominent at low temperatures, close to the melting point of $ZnCl_2$, leading to the formation of abundant micropores, a significant mesopore formation is observed that is due to the partial carbonization and other side reactions at higher temperatures (>400 °C). Evidently, high-temperature synthesis of CTFs in various eutectic salt mixtures of $ZnCl_2$ with alkali metal chloride salts also leads to mesopore formation. We reasoned that using the isocyanate moieties instead of cyano groups in the monomer, 1,4-phenylene isocyanate, could enable efficient interactions between carbonyl moieties and alkali metal ions to realize efficient salt templating to form covalent isocyanurate frameworks (CICFs). In this direction, the trimerization of 1,4-phenylene diisocyanate was carried out under ionothermal conditions at different reaction temperatures using $ZnCl_2$ (CICF) and the eutectic salt mixture of KCl/NaCl/$ZnCl_2$ (CICF-KCl/NaCl) as the reactive solvents. We observed notable differences in the morphologies of the two polymers, whereas CICF showed irregular-shaped micrometer-sized particles, the CICF-KCl/NaCl exhibited a filmlike morphology. Moreover, favorable ion-dipole interactions between alkali metal cations and oxygen atoms of the monomer facilitated two-dimensional growth and the formation of a purely microporous framework in the case of CICF-KCl/NaCl along with a near theoretical retention of the nitrogen content at 500 °C. The CICF-KCl/NaCl showed a BET surface area of 590 $m^2\ g^{-1}$ along with a CO_2 uptake capacity of 5.9 mmol g^{-1} at 273 K and 1.1 bar because of its high microporosity and nitrogen content. On the contrary, in the absence of alkali metal ions, CICF showed high mesopore content and a moderate CO_2 uptake capacity. This study underscores the importance of the strength of the interactions between the salts and the monomer in the ionothermal synthesis to control the morphology, porosity, and gas uptake properties of the porous organic polymers.

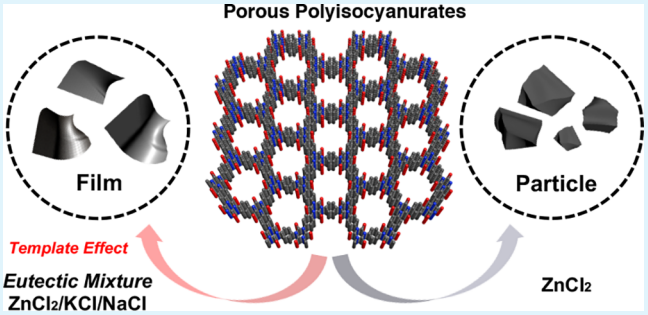

KEYWORDS: *polyisocyanurates, eutectic salts, ionothermal synthesis, template synthesis, gas sorption*

■ INTRODUCTION

Porous organic polymers, POPs,[1−5] have been the subject of intensive research because of their synthetic modularity, chemical stability, high surface areas, and tailor-made surface functionalities for various applications pertaining to chemical separations,[6−8] gas storage,[6,9,10] heterogeneous catalysis,[6,9,11] CO_2 capture and conversion,[6,11−16] water capture,[17] energy conversion,[6] and electrodes for energy storage.[13] Of particular importance are the trimerization reactions of the aromatic nitriles,[18] ethynyls,[19] *ortho*-aminonitriles,[20] isocyanates,[21] and boronic acids[22] for the preparation of POPs.[21,22] For example, the trimerization reaction of aromatic nitriles under ionothermal conditions, first reported by Thomas and Antonietti,[23] using $ZnCl_2$ as a reactive solvent led to the development of covalent triazine frameworks, CTFs. Owing to their conjugated nature, high heteroatom content and tunable porosity, CTFs have already found applications in gas storage,[6,16,24,25] photocatalysis,[26] heterogeneous catalysis,[6,13] energy storage[13] and environmental remediation.[6] The textural properties, crystallinity, and heteroatom content of the CTFs were found to be highly dependent on the reaction temperature as well as the amount of $ZnCl_2$.[18,27,28] In the formation of CTFs, $ZnCl_2$ acts as a Lewis acid for the trimerization of aromatic nitriles through ion-dipole interaction between nitrogen atom and the Zn^{2+} cation. These non-covalent interactions enable a soft templation effect to generate

Scheme 1. Synthesis of Covalent Isocyanurate Frameworks (CICFs) under Ionothermal Reaction Conditions Using $ZnCl_2$ and the Eutectic Mixture of $ZnCl_2$/NaCl/KCl;[a] Right: Graphical Representation of the Proposed CICF Structure

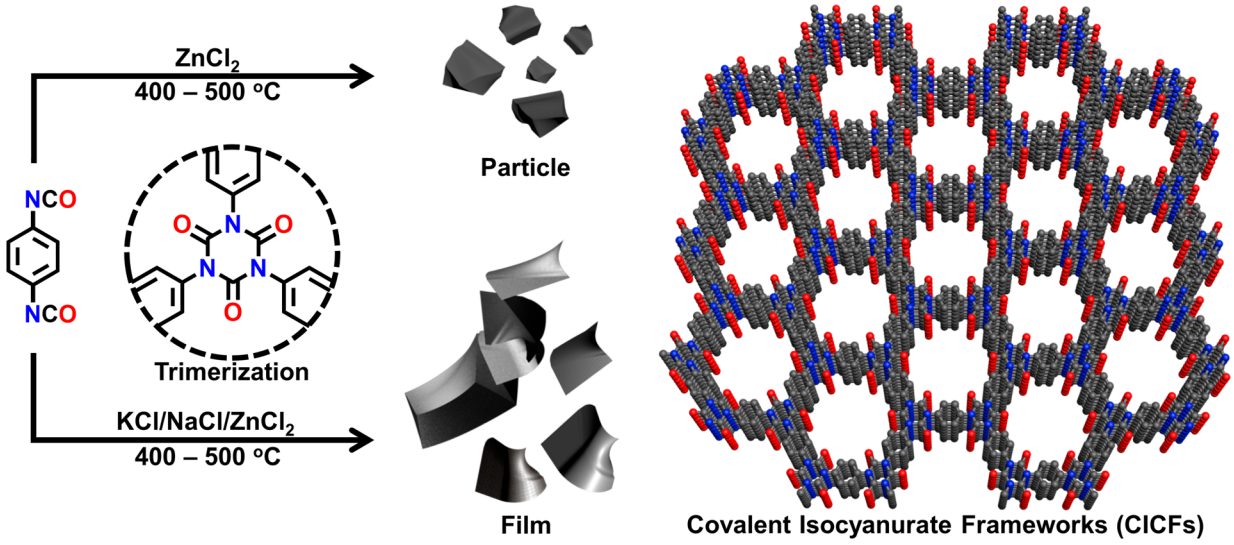

[a]The CICFs showed either particle- or filmlike morphology depending on the synthesis condition.

highly microporous CTFs at low temperatures. Increasing the reaction temperature led to a significant increase in the surface areas and conductivity; however, it was accompanied by a decrease in the crystallinity and a substantial loss in the nitrogen content along with a significant mesopore formation due to the partial carbonization, pointing to the loss of templation effect at high temperatures.[29] In an effort to control the textural properties of CTFs, eutectic mixtures of $ZnCl_2$ with alkali metal chloride salts have also been investigated.[20] The main advantage of this approach is that it lowers the melting point of $ZnCl_2$ to enable the formation of CTFs at lower temperatures. Interestingly, at elevated temperatures, the presence of alkali metal salts led to a significant mesopore formation, which might be explained by the low affinity of the nitrogen atom toward the alkali metal cations.[30] Nevertheless, Lotsch and co-workers recently utilized the eutectic mixture of $ZnCl_2$/NaCl/KCl in the synthesis of polyimide covalent organic frameworks (COFs), thus showing the promising aspect of this method to achieve condensation polymerization at lower temperatures (~250 °C) compared to the $ZnCl_2$ (290 °C).[31]

Following the discovery of polyurethane, isocyanurate linkages used as a cross-linker to tune the properties of polyurethane foams. Aside from this, polyisocyanurates have also found applications as insulators and flame retardants because of their high thermal stability. The cyclotrimerization reaction of three isocyanate molecules is the most atom-efficient, scalable, and practical route for the preparation of polyisocyanurates. Albeit these promising aspects, the reports on the synthesis of porous polyisocyanurates are rather scarce.[21,32] Scherf and co-workers studied the formation of porous organic polymers by using commercially available, aromatic diisocyanates using various catalyst systems including, tetrakis(dimethylamino)ethylene, TDAE, sodium *p*-toluenesulfinate, and TBAF.[21] The resulting materials showed a broad range of porosity varying from nonporous to highly porous with a specific surface area of 1320 m^2 g^{-1} for the sodium *p*-toluenesulfinate catalyzed polymer. The polymers showed significant mesopore content and relatively modest CO_2 uptake capacity of ~3.2 mmol g^{-1} at 273 K, 1 bar. Nevertheless, the monoliths of these polymers also showed interesting lipophilic properties for oil capture. We reasoned that the trimerization reaction of aromatic isocyanates could also be promoted by using Lewis acids through ion-dipole interactions to introduce a templating effect in order to control the morphology and textural properties of resulting POPs. In this direction, we resort to ionothermal reaction involving $ZnCl_2$ and the eutectic salt mixture of $ZnCl_2$/KCl/NaCl at different temperatures to form covalent isocyanurate frameworks (CICFs). The latter approach offers a template effect through the strong noncovalent interactions between O atoms and alkali metal cations to achieve control over morphology and textural properties.

RESULTS AND DISCUSSION

The synthesis of CICF is based on the intermolecular trimerization reaction of 1,4-phenylene diisocyanate to form a planar six-membered isocyanurate ring. Ionothermal synthesis approach involving the molten salts of $ZnCl_2$ and the eutectic salt mixture of $ZnCl_2$/KCl/NaCl has been successfully applied to form polytriazine networks, CTFs, which were found to be reversible at 400 °C, but becomes irreversible at higher temperatures.[33] In particular, the eutectic salt mixture of $ZnCl_2$/KCl/NaCl enables the polymerization reaction to occur at relatively lower temperatures. 1,4-phenylene diisocyanate has a good solubility in these salt-melts and forms clear solutions. CICFs were synthesized (Scheme 1) by the heating of 1,4-phenylene diisocyanate in the molten salts of $ZnCl_2$ and its eutectic mixture $ZnCl_2$/NaCl/KCl at 400 and 500 °C for 24 h in a sealed ampule. We have observed significant differences in the morphology of the resulting polymers; whereas the one synthesized in the $ZnCl_2$(CICF) formed a monolith, we observed the formation of a film in the case of $ZnCl_2$/NaCl/KCl (CICF-KCl/NaCl). For the efficient removal of the metal salts, the samples were crushed into fine powders and then washed thoroughly with water to remove any residual salts. Further stirring in 2 M HCl for 15 h and centrifugation were carried out. After this purification step, the resulting black

powders were washed successively with water, methanol, ethanol, and THF. We choose the optimized mole ratio of 1,4-phenylene diisocyanate: salt (1:5) based on the surface area screening tests (see the Experimental Section). The formation of CICF via the trimerization reaction has been monitored by Fourier-transform infrared spectroscopy (FTIR) measurements. The FTIR spectra of the CICFs and CICFs-KCl/NaCl (Figure 1) revealed the absence of a strong stretching band originating from the isocyanurate (N═C═O) at 2274 cm^{-1} and the concomitant emergence of strong absorption bands at 1303 cm^{-1}, pointing to the formation of six-membered isocyanate rings containing triimide stretching bands and thus indicating the complete intermolecular trimerization of 1,4-phenylene diisocyanate monomers at elevated temperatures.[34,35] It is important to note that there is a slight difference in the FTIR peak position and the shapes of CICFs prepared at different temperatures such as 400 and 500 °C. Interestingly, CICF-KCl/NaCl synthesized at 250 °C does not show the formation of isocyanurate ring and the corresponding isocyanate (N═C═O) stretching band was still present. The formation of isocyanurate ring was observed for the CICFs-KCl/NaCl synthesized at 400 and 500 °C (Figure 1). We also observed a slight red shift for the cyanurate ring stretching in CICF-KCl/NaCl-500 (from 1061 to 1200 cm^{-1}).

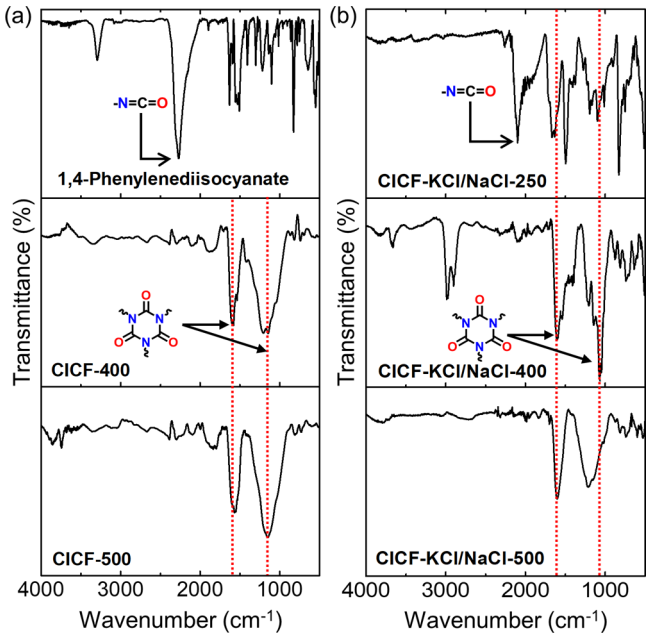

Figure 1. FTIR spectra (a) of the 1,4-phenylene diisocyanate and its trimerization in $ZnCl_2$ (at 400 and 500 °C) and (b) in $ZnCl_2$/KCl/NaCl (at 250, 400, and 500 °C). The characteristic absorption bands for isocynate and isocyanurate ring are highlighted.

Elemental analysis (Table 1) results showed a depletion of nitrogen content with increasing reaction temperature from 400 to 500 °C for CICFs, which agrees well with the CTFs synthesized under ionothermal conditions. Up to 7.8 wt % nitrogen can be preserved for CICFs synthesized at 500 °C. In contrast, the eutectic salt mixture approach led to a 14.1 wt % nitrogen content at 500 °C, which is rather close to the theoretical value of 17.06 wt %. We compared the theoretical C/N ratio with the experimental values obtained for CICF-500 and CICF-KCl/NaCl-500. While the theoretical C/N ratio is 3.43, those of CICF-500 and CICF-KCl/NaCl-500 are 9.9 and 4.6, respectively. The isocyanurate polymers are known[36] to undergo a ring opening reaction to form free isocyanate moieties at 400 °C and subsequent losses of CO_2 and N_2 gases at elevated temperatures (500−600 °C), which was accompanied by carbonization. Accordingly, these results suggest the ability of alkali metal cations to stabilize the isocyanurate rings through ion-dipole interactions and mitigate irreversible side reactions at elevated temperatures. This result is quite significant considering the fact that both CTFs and CICFs suffer from significant loss of nitrogen at temperatures above 400 °C,[18,33] thus underlining the importance of the template effect.

X-ray photoelectron spectroscopy (XPS) analysis was performed to clarify the nature of chemical bonding in CICFs and CICFs-KCl/NaCl. The XPS survey spectrum of CICF-500 and CICF-KCl/NaCl-500, which were selected based on their surface areas, exhibited the peaks of C 1s, N 1s and O 1s and there were no signatures of any other inorganic residues such as Zn, K, Na and Cl. As shown in Figure 2, the C 1s spectra of CICF-500 and CICF-KCl/NaCl-500 were resolved into three components with binding energies of 284.6, 285.8, and 288.5 eV assigned to C═C, C−N, and C═O, respectively.[37] The peaks located at 398.5 and 400.3 eV from the N 1s spectra (Figure 2b, e) of CICF-500 and CICFs-KCl/NaCl-500 depict the N attached with phenyl ring and N bonded with the C═O present in the six-membered isocyanurate ring.[38] Interestingly, in the N 1s spectrum, although the area of C−N was found to be higher than that of O═C−N in the case of CICF-KCl/NaCl-500, the opposite trend was observed for CICF-500, which suggests that the eutectic salt approach can preserve the isocyanurate ring and pore networks through the template effect. The dominant O 1s signals (Figure 2c, f) centered at approximately 532.1 were attributed to O═C−N functional groups present in the

Table 1. BET Surface Area Analysis and Elemental Analysis of CICFs and CICFs-KCl/NaCl

	BET[a], (m^2 g^{-1})	Langmuir (m^2 g^{-1})	d_{micro}[b] (nm)	V_{micro}[c] (cm^3 g^{-1})	S_{micro}[d] (m^2 g^{-1})	S_{ext} (m^2 g^{-1})	V_{total}[e] (cm^3 g^{-1})	EA (wt %) C	N	H
theoretical								58.53[f]	17.06[f]	4.91[f]
CICF-400	657	787	0.5	0.24	566	91	0.32	76.5	9.7	3.72
CICF-500	1674	2022	0.48	0.15	519	1156	0.95	77.2	7.8	3.45
CICF-KCl/NaCl-500	590	683	0.51	0.18	551	39	0.27	64.1	14.1	1.78

[a]Brunauer−Emmett−Teller (BET) surface area calculated over the pressure range (P/P_0) of 0.01−0.11. [b]Micropore diameter calculated from the NLDFT method. [c]Micropore volume calculated using the *t*-plot method. [d]Micropore surface calculated using the *t*-plot method. [e]Total pore volume obtained at P/P_0 = 0.99. [f]Theoretical elemental analysis (EA) value calculated for $C_{24}H_{24}N_6O_6$.

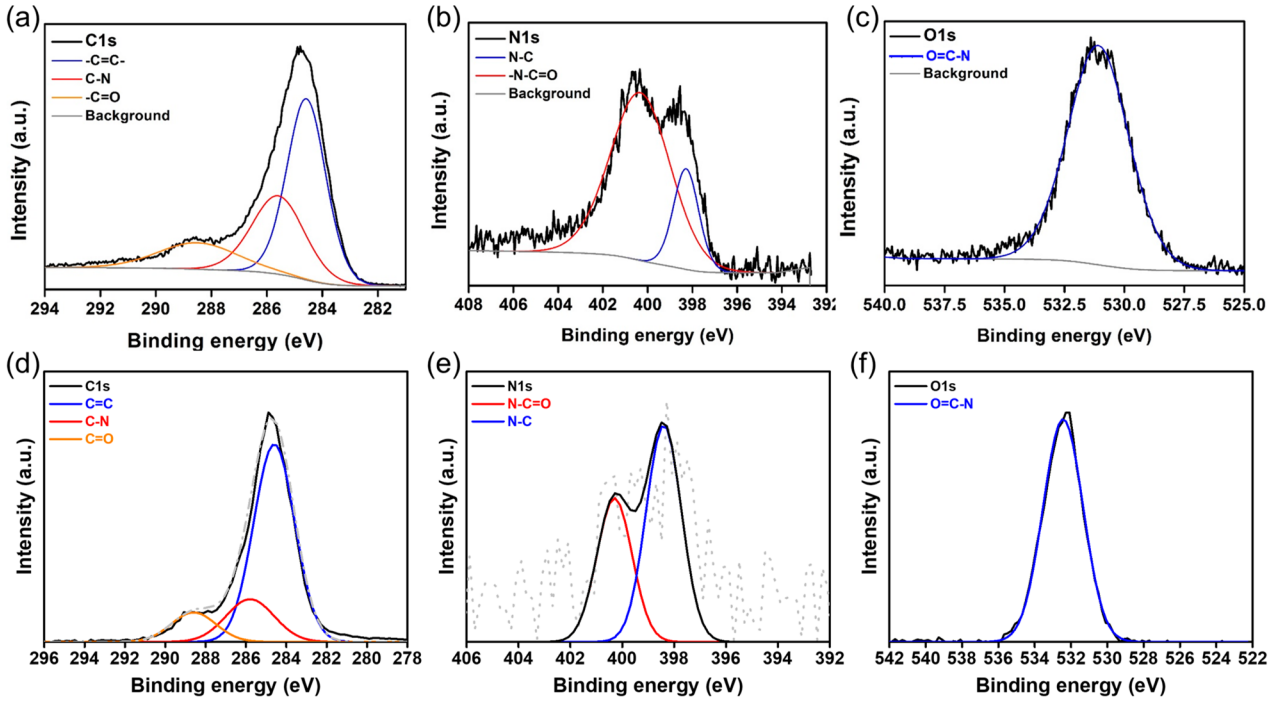

Figure 2. Deconvoluted XPS spectra for C 1s, N 1s, and O 1s of (a–c) CICF-500 and of (d–f) CICF-KCl/NaCl-500.

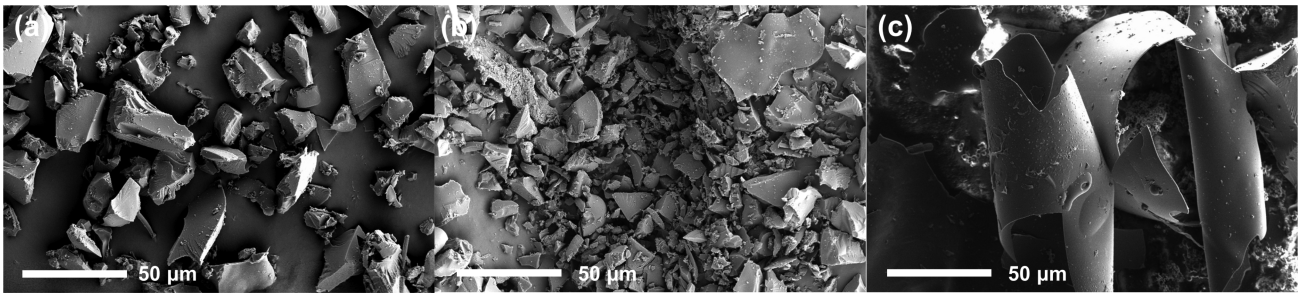

Figure 3. SEM images of (a) CICF-400, (b) CICF-500, and (c) CICF-KCl/NaCl-500. The eutectic salt mixture ($ZnCl_2$/KCl/NaCl) leads to the formation of a filmlike morphology through a salt templating effect.

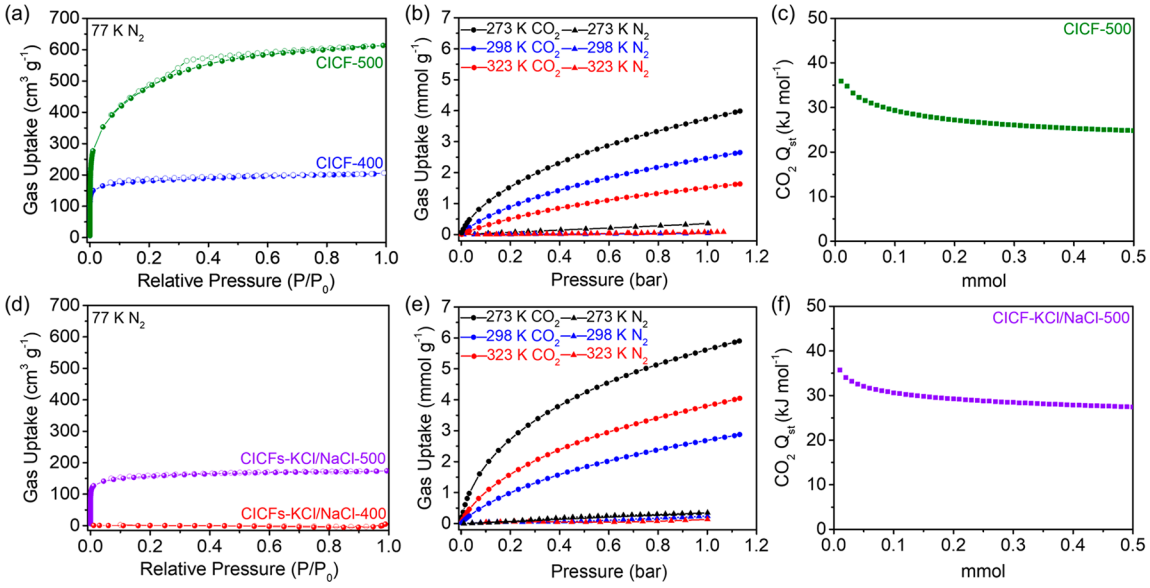

Figure 4. BET isotherm of (a) CICFs and (d) CICFs-KCl/NaCl. CO_2 uptake of (b) CICF-500 and (e) CICF-KCl/NaCl-500. CO_2 heat of adsorption (Q_{st}) of (c) CICF-500 and (f) CICF-KCl/NaCl-500.

Table 2. CO_2 and N_2 Uptake Capacities of CICF-500 and CICFs-KCl/NaCl-500 at 273, 298, and 323 K along with the CO_2 Isosteric Heats of Adsorption Values

	CO_2 at 1.1 bar (mmol g^{-1})				N_2 at 1.1 bar (mmol g^{-1})		
	273 K	298 K	323 K	Q_{st} at zero coverage[a] (kJ mol^{-1})	273 K	298 K	323 K
CICF-500	3.95	2.63	1.62	35.83 (25.31)[b]	0.36	0.044	0.084
CICF-KCl/NaCl-500	5.90	4.04	2.87	35.87 (27.93)[b]	0.35	0.24	0.13

[a]Isosteric heat of adsorption (Q_{st}) values were calculated by using the Clausius−Clapeyron equation. [b]Q_{st} values at high loadings.

CICFs.[37] These results support the formation and stabilization of isocyanurate rings within the CICFs.

The morphology of the CICFs were probed by scanning electron microscopy (SEM) analysis (Figure 3). We observed significant differences between CICFs and CICFs-KCl/NaCl. Although CICF exhibited irregular shaped micrometer-size particles, CICFs-KCl/NaCl showed filmlike morphology. The wrinkled morphology is clearly observed on the top-view of this film (Figure S1) compared to monolithic crude of CICFs (Figure S2). We believe that the template effect originating from the alkali metal cations promote the two-dimensional growth to form a filmlike morphology, possibly at the liquid−gas interface. Powder X-ray diffraction (PXRD) analysis of CICFs (CICF-400 and CICF-500) showed their amorphous nature (Figure S3a, b). The broad diffraction peak located at 2θ = 25.7°, which is assigned to the (001) basal plane diffraction peak, suggests the existence of graphitic layers with an interlayer distance of around 3.4 Å.[39] However, CICFs-KCl/NaCl showed an improved semicrystalline pattern (Figure S3c, d). CICF-KCl/NaCl-400 exhibited an intense peak at low angles, consistent with the PXRD patterns of CTF-1 and COF nanosheets obtained in the presence of table salt.[23,40]

To investigate the textural properties of CICFs and CICFs-KCl/NaCl, we measured N_2 adsorption−desorption isotherms at 77 K (Figure 4, Figure S4 and S5, and Table S1). As shown in Figure 4a, 4d, all of the CICFs showed typical type I isotherms, indicating a well-developed micropore formation at 400 °C. The difference in the porosity of CICF and CICF-KCl/NaCl became more apparent at 500 °C. CICF-KCl/NaCl maintained its microporous structure, but we observed a significant mesopore formation evidenced by the presence of H4 hysteresis in the desorption branch in the case of CICF-500, in line with the previously reported CTFs synthesized at high temperatures.[33] The Brunauer−Emmett−Teller (BET) model, in which the valid pressure ranges were obtained from the Rouquerol plots (Figures S6−S10), was applied to the isotherm, which resulted in apparent surface areas of 657, 1674, and 590 m^2 g^{-1} and a pore volumes of 0.32, 0.95, and 0.27 cm^3 g^{-1} (Table 1) for CICF-400, CICF-500, and CICF-KCl/NaCl-500, respectively. We attributed the higher surface area of CICF-500 compared to that of CICF-KCl/NaCl-500 to the significant mesopore formation originating from irreversible side reactions and partial carbonization at 500 °C. CICFs-KCl/NaCl-250 and -400 were found to be nonporous, presumably because of the lack of accessibility of the pores and incomplete polymerization in the case of the former. We analyzed the pore size distribution of CICFs using the NLDFT model from N_2 adsorption data at 77 K (N_2 at 77 K carbon standard slit model) and BJH (Barrett−Joyner−Halenda) methods (Figure S11). The fitting errors between experimental N_2 adsorption isotherm and the calculated NLDFT isotherm were found to be below 1%, at 0.60, 0.97, and 0.94% for CICF-400, CICF-500, and CICF-KCl/NaCl-500, respectively (Figure S12). CICF-400 showed two types of pores with the size of 0.5 and 1.1 nm with almost no mesoporosity. On the other hand, CICF-500 showed micropores in the range of 0.48 to 1.13 nm and mesopores in the range of 3 to 15 nm. Similar to the CTFs,[28,33] we attribute the mesopore formation to the partial carbonization at this temperature range. We also observed similar micropore surface areas for CICF-400 and CICF-500 (Table 1). CICF-KCl/NaCl-500 exhibited (Figure 4d, Figure S11, and Table 1) two maxima at 0.51 and 1.1 nm in the pore size distribution. While the larger pore is attributed to the hexagonal pores of CICF, the smaller one could originate from the stacking of 2D sheets. This result clearly shows that even at 500 °C, the template effect of KCl/NaCl promotes the microporosity accompanied by a significant retention in the nitrogen content.

To compare the CO_2 affinity of CICF and of CICF-KCl/NaCl, we performed CO_2 uptake experiments at 273, 298, and 323 K up to 1.1 bar for CICF-500 and CICF-KCl/NaCl (Figure 4 and Table 2). CICF-500 showed 3.95 mmol g^{-1} of CO_2 at 1.1 bar, whereas CICF-KCl/NaCl-500 showed 5.9 mmol g^{-1} of CO_2 at 1.1 bar (Figure 4b, e) and Table S2), 273 K. The significant difference in CO_2 uptake capacities is attributed to the combination of solely microporous structure and almost two-times higher nitrogen content (14.1 wt %) of CICF-KCl/NaCl-500 compared to CICF-500. The CO_2 heat of adsorption (Q_{st}) of CO_2 was found (Table 2) to be 35.83 and 35.87 kJ mol^{-1} for CICF-500 and CICF-KCl/NaCl-500 at zero coverage, respectively. However, the CO_2 Q_{st} of CICF-KCl/NaCl-500 (Figure S13) exhibits a significantly higher value than the one for CICF-500 at high loadings. We attribute this result to the higher nitrogen content of CICF-KCl/NaCl-500 compared to CICF-500 (14.1 wt % CICF-KCl/NaCl-500 and 7.8 wt % CICF-500). Interestingly, whereas CICF-400 and CICF-KCl/NaCl-500 have almost similar N_2 adsorption−desorption isotherms (Figure 4 and Table S1) with comparable BET surface areas of 657 m^2 g^{-1} for CICF-400 and 590 m^2 g^{-1} for CICF-KCl/NaCl-500, CICF-400 showed only 1.63 mmol g^{-1} of CO_2 uptake at 1.1 bar, 273 K, which further verifies the impact of favorable textural properties and higher heteroatom content in the case of CICF-KCl/NaCl-500. Moreover, the stabilization of isocyanurate rings through the template effect enables high nitrogen retention even at 500 °C, thus providing an ideal platform for efficient CO_2 capture.

■ CONCLUSION

We demonstrated atom-efficient and facile synthesis of porous polyisocyanurates through the cyclotrimerization reaction of triisocyanate molecules under ionothermal and eutectic salt mixture conditions. Comparative analysis of reaction conditions revealed the strong template effect originating from the presence of alkali metal salts in the salt-melt mixture. This template effect provides a useful tool to tune the textural properties, morphology, and gas uptake properties of the

resulting porous organic polymers. Notably, the stabilization of isocyanurate rings through the noncovalent interactions enabled not only two-dimensional growth to form a film-like morphology, but also near theoretical retention of the nitrogen content at elevated temperatures, thus possibly extending the application of these polymers to membranes, energy storage, and catalysis.

EXPERIMENTAL SECTION

Materials. 1,4-Phenylene diisocyanate, potassium chloride (KCl), sodium chloride (NaCl) and anhydrous $ZnCl_2$ were purchased from Sigma-Aldrich and used as received.

Synthesis of Covalent Isocyanurate Frameworks (CICFs). CICF was synthesized by the cyclotrimerization of 1,4-phenylene diisocyanate in molten $ZnCl_2$ at 400 and 500 °C. To identify the optimal $ZnCl_2$ amount for the synthesis of CICFs, we varied (1,4-phenylene diisocyanate: $ZnCl_2$ equivalent ratio of 1:5, and 1:10) the $ZnCl_2$ equivalent ratio with respect to 1,4-phenylene diisocyanate. Monomer: $ZnCl_2$ ratio of 1:5 was identified as the optimal condition based on the higher specific surface areas of the resulting CICF materials (Figures S4 and S6−S12 and Table S1).

In a typical synthesis, 0.5 g of 1,4- phenylene diisocyanate and 2.12 g (1:5 equiv.) or 4.24 g (1:10 equiv.) of the $ZnCl_2$ were transferred into a Pyrex ampule (3 × 12 cm) under an inert atmosphere. The ampules were evacuated and sealed at room temperature. The ampules were transferred into a box furnace and temperature was raised to 400 or 500 °C (3 °C min^{-1} heating rate) and kept it under these conditions for 24 h in order to obtain CICFs. The ampule was then cooled to room temperature and opened carefully. The black-colored CICFs samples were subsequently grounded into fine powders and washed thoroughly with water to remove most of the $ZnCl_2$. Further stirring in 2 M HCl for 15 h and centrifugation step was carried out to remove the residual salt. After this purification step, the resulting black powder was washed successively with water, methanol, ethanol, and THF and dried in a vacuum oven at 100 °C for 24 h.

Synthesis of Covalent Isocyanurate Frameworks in the Salt Mixture (CICFs-KCl/NaCl). The mixture of KCl/NaCl was ball milled to obtain homogeneity with micrometer-sized particles. Afterwards, the eutectic salt mixture of anhydrous zinc chloride:potassium chloride:sodium chloride equivalent mole ratio of 3.95:2.52:1 was prepared. CICFs-KCl/NaCl was synthesized using a 1,4-phenylene diisocyanate:salt ratio of 1:5 by following the same procedure as above at 250, 400, 500 °C.

Characterization Methods. The powder X-ray diffraction (PXRD) patterns of CICFs and CICFs-KCl/NaCl were collected on a Rigaku D/MAX-2500 (18 kW) micro area X-ray diffractometer using CuKα (k = 0.154 nm) radiation. The X-ray diffractograms were recorded in the 2θ range of 5−60 with a 2θ step size of 0.15 and a step time of 1 s. The morphology of CICFs and CICFs-KCl/NaCl was investigated using a field-emission scanning electron microscope (FE-SEM, Sirion). Detailed characterization of various chemical bonds in each sample were characterized by Fourier-transform infrared spectroscopy (FTIR, Bruker) by preparing KBr pellets. X-ray photoelectron spectroscopy (XPS) analysis was performed with a multipurpose XPS (Sigma Probe, Thermo VG Scientific, X-ray Source: monochromatic Al K(alpha)). Elemental analysis of CICFs and CICFs-KCl/NaCl was carried out by using a FlashEA 2000 (Series) [C, H, N, S] Elemental Analyzer). The textural parameters of CICFs and CICFs-KCl/NaCl were evaluated by using N_2 adsorption and desorption isotherms, which were measured at 77 K on a Micrometrics 3Flex surface characterization analyzer. All samples were outgassed at 120 °C for 16 h prior to the analysis. The specific surface areas of samples were calculated using the BET and Langmuir model in the pressure range where the term $V(1 - P/P_0)$ continuously increases with P/P_0 in the Rouquerol plot. The pore size distributions (PSD) of samples were calculated from nitrogen isotherms at 77 K according to the nonlocal density functional theory (NLDFT) method (calculated model: carbon standard slit) and the Barrett−Joyner−Halenda (BJH) method with Harkins and Jura thickness curve. The low-pressure CO_2 and N_2 adsorption isotherms of samples were recorded on a Micrometrics 3Flex instrument at three different temperatures of 273, 298, and 323 K. The circulator was used to keep the temperature constant during adsorption/desorption analysis. Isosteric heat of absorption (Q_{st}) values were calculated by using the standard calculation routine, that is, the Clausius−Clapeyron equation, in *Mathematica* software.

ASSOCIATED CONTENT

Supporting Information

The Supporting Information is available free of charge at https://pubs.acs.org/doi/10.1021/acsami.1c06326.

Additional structural and spectroscopic data (PDF)

AUTHOR INFORMATION

Corresponding Author

Ali Coskun − *Department of Chemistry, University of Fribourg, Fribourg 1700, Switzerland;* orcid.org/0000-0002-4760-1546; Email: ali.coskun@unifr.ch

Authors

Kyung Seob Song − *Department of Chemistry, University of Fribourg, Fribourg 1700, Switzerland*

Siddulu Naidu Talapaneni − *Australian Carbon Materials Centre (A-CMC), School of Chemical Engineering, University of New South Wales (UNSW), Sydney, New South Wales 2052, Australia;* orcid.org/0000-0002-7684-7529

Timur Ashirov − *Department of Chemistry, University of Fribourg, Fribourg 1700, Switzerland*

Complete contact information is available at: https://pubs.acs.org/10.1021/acsami.1c06326

Author Contributions

The manuscript was written through contributions of all authors and all authors have given approval to the final version of the manuscript.

Notes

The authors declare no competing financial interest.

ACKNOWLEDGMENTS

We acknowledge the support from the Swiss National Science Foundation (SNF) for funding of this research (200021-175947).

REFERENCES

(1) Chaoui, N.; Trunk, M.; Dawson, R.; Schmidt, J.; Thomas, A. Trends and Challenges for Microporous Polymers. *Chem. Soc. Rev.* **2017**, *46* (11), 3302−3321.

(2) Das, S.; Heasman, P.; Ben, T.; Qiu, S. Porous Organic Materials: Strategic Design and Structure-Function Correlation. *Chem. Rev.* **2017**, *117* (3), 1515−1563.

(3) Diercks, C. S.; Yaghi, O. M. The Atom, the Molecule, and the Covalent Organic Framework. *Science* **2017**, *355* (6328), eaal1585.

(4) Lee, J.-S. M.; Cooper, A. I. Advances in Conjugated Microporous Polymers. *Chem. Rev.* **2020**, *120* (4), 2171−2214.

(5) Haase, F.; Lotsch, B. V. Solving the COF Trilemma: Towards Crystalline, Stable and Functional Covalent Organic Frameworks. *Chem. Soc. Rev.* **2020**, *49* (23), 8469−8500.

(6) Krishnaraj, C.; Jena, H. S.; Leus, K.; Van Der Voort, P. Covalent Triazine Frameworks-A Sustainable Perspective. *Green Chem.* **2020**, *22* (4), 1038−1071.

(7) Wang, Z.; Zhang, S.; Chen, Y.; Zhang, Z.; Ma, S. Covalent Organic Frameworks for Separation Applications. *Chem. Soc. Rev.* **2020**, *49* (3), 708−735.
(8) Yin, C.; Zhang, Z.; Zhou, J.; Wang, Y. Single-Layered Nanosheets of Covalent Triazine Frameworks (CTFs) by Mild Oxidation for Molecular-Sieving Membranes. *ACS Appl. Mater. Interfaces* **2020**, *12* (16), 18944−18951.
(9) Sadak, A. E.; Karakus, E.; Chumakov, Y. M.; Dogan, N. A.; Yavuz, C. T. Triazatruxene-Based Ordered Porous Polymer: High Capacity CO2, CH4, and H2 Capture, Heterogeneous Suzuki-Miyaura Catalytic Coupling, and Thermoelectric Properties. *ACS Appl. Energy Mater.* **2020**, *3* (5), 4983−4994.
(10) Che, S.; Pang, J.; Kalin, A. J.; Wang, C.; Ji, X.; Lee, J.; Cole, D.; Li, J.-L.; Tu, X.; Zhang, Q.; et al. Rigid Ladder-type Porous Polymer Networks for Entropically Favorable Gas Adsorption. *ACS Mater. Lett.* **2020**, *2* (1), 49−54.
(11) Kaur, P.; Hupp, J. T.; Nguyen, S. T. Porous Organic Polymers in Catalysis: Opportunities and Challenges. *ACS Catal.* **2011**, *1* (7), 819−835.
(12) Zou, L.; Sun, Y.; Che, S.; Yang, X.; Wang, X.; Bosch, M.; Wang, Q.; Li, H.; Smith, M.; Yuan, S.; et al. Porous Organic Polymers for Post-combustion Carbon Capture. *Adv. Mater.* **2017**, *29* (37), 1700229.
(13) Liu, M.; Guo, L.; Jin, S.; Tan, B. Covalent Triazine Frameworks: Synthesis and Applications. *J. Mater. Chem. A* **2019**, *7* (10), 5153−5172.
(14) Nguyen, T. S.; Yavuz, C. T. Quantifying the Nitrogen Effect on CO2 Capture using Isoporous Network Polymers. *Chem. Commun.* **2020**, *56* (31), 4273−4275.
(15) Ashourirad, B.; Arab, P.; Verlander, A.; El-Kaderi, H. M. From Azo-linked Polymers to Microporous Heteroatom-doped Carbons: Tailored Chemical and Textural Properties for Gas Separation. *ACS Appl. Mater. Interfaces* **2016**, *8* (13), 8491−8501.
(16) Wang, K.; Huang, H.; Liu, D.; Wang, C.; Li, J.; Zhong, C. Covalent Triazine-based Frameworks with Ultramicropores and High Nitrogen Contents for Highly Selective CO2 Capture. *Environ. Sci. Technol.* **2016**, *50* (9), 4869−4876.
(17) Byun, Y.; Je, S. H.; Talapaneni, S. N.; Coskun, A. Advances in Porous Organic Polymers for Efficient Water Capture. *Chem. - Eur. J.* **2019**, *25* (44), 10262−10283.
(18) Kuhn, P.; Antonietti, M.; Thomas, A. Porous, Covalent Triazine-Based Frameworks Prepared by Ionothermal Synthesis. *Angew. Chem., Int. Ed.* **2008**, *47* (18), 3450−3453.
(19) Yuan, S.; Dorney, B.; White, D.; Kirklin, S.; Zapol, P.; Yu, L.; Liu, D.-J. Microporous Polyphenylenes with Tunable Pore Size for Hydrogen Storage. *Chem. Commun.* **2010**, *46* (25), 4547−4549.
(20) Buyukcakir, O.; Yuksel, R.; Jiang, Y.; Lee, S. H.; Seong, W. K.; Chen, X.; Ruoff, R. S. Synthesis of Porous Covalent Quinazoline Networks (cqns) and their Gas Sorption Properties. *Angew. Chem., Int. Ed.* **2019**, *58* (3), 872−876.
(21) Preis, E.; Schindler, N.; Adrian, S.; Scherf, U. Microporous Polymer Networks made by Cyclotrimerization of Commercial, Aromatic Diisocyanates. *ACS Macro Lett.* **2015**, *4* (11), 1268−1272.
(22) Cote, A. P.; Benin, A. I.; Ockwig, N. W.; O'Keeffe, M.; Matzger, A. J.; Yaghi, O. M. Porous, Crystalline, Covalent Organic Frameworks. *Science* **2005**, *310* (5751), 1166−1170.
(23) Kuhn, P.; Antonietti, M.; Thomas, A. Porous, Covalent Triazine-Based Frameworks Prepared by Ionothermal Synthesis. *Angew. Chem., Int. Ed.* **2008**, *47* (18), 3450−3453.
(24) Wang, H.; Jiang, D.; Huang, D.; Zeng, G.; Xu, P.; Lai, C.; Chen, M.; Cheng, M.; Zhang, C.; Wang, Z. Covalent Triazine Frameworks for Carbon Dioxide Capture. *J. Mater. Chem. A* **2019**, *7* (40), 22848−22870.
(25) Lee, Y. J.; Talapaneni, S. N.; Coskun, A. Chemically Activated Covalent Triazine Frameworks with Enhanced Textural Properties for High Capacity Gas Storage. *ACS Appl. Mater. Interfaces* **2017**, *9* (36), 30679−30685.
(26) Qian, Z.; Wang, Z. J.; Zhang, K. A. Covalent Triazine Frameworks as Emerging Heterogeneous Photocatalysts. *Chem. Mater.* **2021**, *33* (6), 1909−1926.
(27) Katekomol, P.; Roeser, J. r. m.; Bojdys, M.; Weber, J.; Thomas, A. Covalent Triazine Frameworks Prepared from 1, 3, 5-Tricyanobenzene. *Chem. Mater.* **2013**, *25* (9), 1542−1548.
(28) Kuhn, P.; Thomas, A.; Antonietti, M. Toward Tailorable Porous Organic Polymer Networks: a High-temperature Dynamic Polymerization Scheme based on Aromatic Nitriles. *Macromolecules* **2009**, *42* (1), 319−326.
(29) Li, Y.; Zheng, S.; Liu, X.; Li, P.; Sun, L.; Yang, R.; Wang, S.; Wu, Z. S.; Bao, X.; Deng, W. Q. Conductive Microporous Covalent Triazine-Based Framework for High-Performance Electrochemical Capacitive Energy Storage. *Angew. Chem.* **2018**, *130* (27), 8124−8128.
(30) Troschke, E.; Grätz, S.; Borchardt, L.; Haubold, D.; Senkovska, I.; Eychmueller, A.; Kaskel, S. Salt Templated Synthesis of Hierarchical Covalent Triazine Frameworks. *Microporous Mesoporous Mater.* **2017**, *239*, 190−194.
(31) Maschita, J.; Banerjee, T.; Savasci, G.; Haase, F.; Ochsenfeld, C.; Lotsch, B. V. Ionothermal Synthesis of Imide-Linked Covalent Organic Frameworks. *Angew. Chem., Int. Ed.* **2020**, *59* (36), 15750−15758.
(32) Zhang, Y.; Riduan, S. N.; Ying, J. Y. Microporous Polyisocyanurate and its Application in Heterogeneous Catalysis. *Chem. - Eur. J.* **2009**, *15* (5), 1077−1081.
(33) Kuhn, P.; Forget, A.; Su, D.; Thomas, A.; Antonietti, M. From Microporous Regular Frameworks to Mesoporous Materials with Ultrahigh Surface Area: Dynamic Reorganization of Porous Polymer Networks. *J. Am. Chem. Soc.* **2008**, *130* (40), 13333−13337.
(34) Dey, S. K.; de Sousa Amadeu, N.; Janiak, C. Microporous Polyurethane Material for Size Selective Heterogeneous Catalysis of the Knoevenagel Reaction. *Chem. Commun.* **2016**, *52* (50), 7834−7837.
(35) Jung, Y. C.; Muramatsu, H.; Hayashi, T.; Kim, J. H.; Kim, Y. A.; Endo, M.; Dresselhaus, M. S. Covalent Attachment of Aromatic Diisocyanate to the Sidewalls of Single- and Double-Walled Carbon Nanotubes. *Eur. J. Inorg. Chem.* **2010**, *2010* (27), 4305−4308.
(36) Jiricny, J.; Reese, C. B. The Thermal Decomposition of Isocyanurates. *Br. Polym. J.* **1980**, *12* (3), 81−84.
(37) Talapaneni, S. N.; Lee, J. H.; Je, S. H.; Buyukcakir, O.; Kwon, T. w.; Polychronopoulou, K.; Choi, J. W.; Coskun, A. Chemical Blowing Approach for Ultramicroporous Carbon Nitride Frameworks and Their Applications in Gas and Energy Storage. *Adv. Funct. Mater.* **2017**, *27* (1), 1604658.
(38) Do, S.; Kwon, W.; Rhee, S.-W. Soft-template Synthesis of Nitrogen-doped Carbon Nanodots: Tunable Visible-Light Photoluminescence and Phosphor-based Light-emitting Diodes. *J. Mater. Chem. C* **2014**, *2* (21), 4221−4226.
(39) Buyukcakir, O.; Je, S. H.; Talapaneni, S. N.; Kim, D.; Coskun, A. Charged Covalent Triazine Frameworks for CO2 Capture and Conversion. *ACS Appl. Mater. Interfaces* **2017**, *9* (8), 7209−7216.
(40) Shi, X.; Ma, D.; Xu, F.; Zhang, Z.; Wang, Y. Table-salt Enabled Interface-confined Synthesis of Covalent Organic Framework (COF) Nanosheets. *Chem. Sci.* **2020**, *11* (4), 989−996.